ECM stiffness primes the TGFβ pathway to promote chondrocyte differentiation

Jessica L. Allen[a,b], Margaret E. Cooke[b,c], and Tamara Alliston[a,b,c,d]
[a]UC Berkeley–UCSF Graduate Program in Bioengineering, [b]Department of Orthopaedic Surgery, [c]School of Medicine, and [d]Department of Bioengineering and Therapeutic Sciences, Department of Otolaryngology–Head and Neck Surgery, and Eli and Edythe Broad Center of Regeneration Medicine and Stem Cell Research, University of California, San Francisco, San Francisco, CA 94143

ABSTRACT **Cells encounter physical cues such as extracellular matrix (ECM) stiffness in a microenvironment replete with biochemical cues. However, the mechanisms by which cells integrate physical and biochemical cues to guide cellular decision making are not well defined. Here we investigate mechanisms by which chondrocytes generate an integrated response to ECM stiffness and transforming growth factor β (TGFβ), a potent agonist of chondrocyte differentiation. Primary murine chondrocytes and ATDC5 cells grown on 0.5-MPa substrates deposit more proteoglycan and express more Sox9, Col2α1, and aggrecan mRNA relative to cells exposed to substrates of any other stiffness. The chondroinductive effect of this discrete stiffness, which falls within the range reported for articular cartilage, requires the stiffness-sensitive induction of TGFβ1. Smad3 phosphorylation, nuclear localization, and transcriptional activity are specifically increased in cells grown on 0.5-MPa substrates. ECM stiffness also primes cells for a synergistic response, such that the combination of ECM stiffness and exogenous TGFβ induces chondrocyte gene expression more robustly than either cue alone through a p38 mitogen-activated protein kinase–dependent mechanism. In this way, the ECM stiffness primes the TGFβ pathway to efficiently promote chondrocyte differentiation. This work reveals novel mechanisms by which cells integrate physical and biochemical cues to exert a coordinated response to their unique cellular microenvironment.**

Monitoring Editor
Kunxin Luo
University of California, Berkeley

Received: Mar 2, 2012
Revised: Jul 11, 2012
Accepted: Jul 19, 2012

INTRODUCTION

The extracellular microenvironment is rich in physical cues that, like biochemical cues, are powerful regulators of cell behavior. Cells respond to physical cues, such as topography, mechanical stimulation, and extracellular matrix (ECM) stiffness, with changes in cell proliferation, migration, apoptosis, and differentiation (Chen *et al.*, 1997; Engler *et al.*, 2006; Wang and Thampatty, 2006; Assoian and Klein, 2008; Geiger *et al.*, 2009). The importance of ECM stiffness in cell fate selection is apparent in mesenchymal stem cells, which select a neural lineage when cultured on a compliant matrix (1 kPa) but differentiate into myotubes on a stiffer matrix (10 kPa; Engler *et al.*, 2006). Therefore, just as morphogen gradients define boundaries and prime cells for lineage selection and differentiation, ECM stiffness refines cellular behavior to match the physical microenvironment. Although cells encounter biochemical and physical cues simultaneously, the mechanisms by which this information is assimilated to direct cellular responses remain unclear.

Cells maintain homeostasis between ECM stiffness and cytoskeletal tension through a tightly controlled hierarchical mechanotransduction pathway. Upon integrin binding to ECM ligands and the generation of internal cell tension, cells develop focal adhesions, a highly ordered array of proteins including focal adhesion kinase (FAK), talin, vinculin, and α-actinin (Miranti and Brugge, 2002; Geiger *et al.*, 2009; Kanchanawong *et al.*, 2010). These proteins interact with small GTPases (i.e., Rho, Rac) and other

This article was published online ahead of print in MBoC in Press (http://www.molbiolcell.org/cgi/doi/10.1091/mbc.E12-03-0172) on July 25, 2012.
Address correspondence to: Tamara Alliston (tamara.alliston@ucsf.edu).

Abbreviations used: Col2α1, collagen, type II, alpha 1; ECM, extracellular matrix; MAPK, mitogen-activated protein kinase; OA, osteoarthritis; ROCK, Rho-associated protein kinase; TGFβ, transforming growth factor beta.

signaling pathways, facilitating changes in cytoskeletal organization, actinomyosin contractility, and cell shape with even small changes in matrix compliance (Paszek *et al.*, 2005; Geiger *et al.*, 2009). Accordingly, distortion of normal ECM stiffness has been implicated in many diseases, including cancer and liver fibrosis (Paszek *et al.*, 2005; Li *et al.*, 2007; Butcher *et al.*, 2009).

Cells integrate their response to physical and biochemical cues to guide cellular decision making. Physical cues, including substrate stiffness, cell shape, or cytoskeletal tension, can radically alter the cellular response to growth factors (Gao *et al.*, 2010; Park *et al.*, 2011; Leight *et al.*, 2012; Wang *et al.*, 2012). For example, insufficient cytoskeletal tension impairs bone morphogenetic protein (BMP)–induced osteogenesis, which is sensitive to the activity of Rho, an integral part of the mechanotransduction pathway (Wang *et al.*, 2012). Among the many effectors shared by biochemical and mechanotransduction pathways, integrins are a prime example of molecules that functionally interact with the ECM and the cytoskeleton, as well as with growth factors and their receptors (Miranti and Brugge, 2002; Munger and Sheppard, 2011). ECM stiffness and transforming growth factor β (TGFβ) signaling can each direct the localization and activity of the transcriptional coregulator TAZ (Varelas *et al.*, 2008; Dupont *et al.*, 2011). Nonetheless, the molecular mechanisms by which cells generate an integrated response to biochemical and physical cues are not well defined.

As a tissue with a primarily mechanical function—cushioning joint surfaces—cartilage is an ideal model for exploring the interaction between physical and biochemical cues. From development—in which cellular condensations drive mesenchymal precursors to select a chondrogenic lineage—to disease—in which osteoarthritis (OA) causes the coupled degeneration of cartilage physical and biochemical properties—this tissue is replete with examples of intersecting physical and biochemical cues (Setton *et al.*, 1999; Aigner *et al.*, 2002; Henderson and Carter, 2002; Shieh and Athanasiou, 2003). Physical properties of cartilage matrix are carefully defined spatially and temporally, facilitating the mechanical and biological functions of this tissue. The stiffness of cartilage ECM varies with development (up to threefold increase from fetal to adult cartilage; Williamson *et al.*, 2001), location (fivefold increase through tissue depth and up to threefold increase from pericellular to interterritorial matrix; Akizuki *et al.*, 1986; Setton *et al.*, 1999; Darling *et al.*, 2010), and disease (twofold decrease in late-stage OA; Kleemann *et al.*, 2005). In addition to a mechanical role at the tissue level, we hypothesize that, at a cellular level, the stiffness of cartilage ECM plays a key role in directing chondrocyte differentiation and homeostasis, possibly by regulating other signaling pathways that control chondrogenesis.

The growth factor TGFβ plays a major role in the regulation of chondrogenesis. TGFβ induces chondrocyte lineage selection and cartilage matrix synthesis while inhibiting terminal chondrocyte differentiation and hypertrophy (Blaney Davidson *et al.*, 2007; Derynck *et al.*, 2008). The TGFβ pathway is regulated at multiple hierarchical levels, several of which intersect with the mechanotransduction pathway. The conversion of the TGFβ ligand from a latent to an active form can occur by proteolytic cleavage, integrin-mediated activation, and cell-generated tension (Munger *et al.*, 1999; Annes *et al.*, 2003; Wipff *et al.*, 2007). Once activated, the ligands signal through a heterotetrameric complex consisting of two type I and two type II serine/threonine kinase receptors, the availability and clustering of which are also tightly controlled (Massague, 1998). Signaling within the cell can be relayed through many different pathways, including Rho/Rho-associated protein kinase (ROCK) and mitogen-activated protein kinase (MAPK) pathways, but the "canonical" effectors of TGFβ signaling are the R-Smads 2 and 3 and the common mediator Smad4 (Wrana, 2000). Even before phosphorylation by TGFβ receptors, localization and stability of Smad2 and Smad3 are regulated through interactions with multiple proteins, including microtubules, filamin, and ubiquitin ligases (Dong *et al.*, 2000; Lin *et al.*, 2000; Sasaki *et al.*, 2001; Zhang *et al.*, 2001). The activated TβRI phosphorylates Smad2 and Smad3 on the C-terminal domain, causing heteromerization with Smad4 and preferential retention in the nucleus, where Smads act as transcription factors. For example, in chondrocytes, phosphorylated Smad3 recruits CBP to activate Sox9-mediated transcription of Col2α1 (Furumatsu *et al.*, 2005).

TGFβ and mechanotransduction share many effectors and regulate many of the same cellular processes. However, the mechanisms by which signaling between these two pathways is integrated are not well defined in chondrocytes or other cell types. Although a recent study highlights this integration in epithelial mesenchymal transition in the context of cancer (Leight *et al.*, 2012), these mechanisms may operate in other diseases where both ECM stiffness and TGFβ have already been implicated individually, such as liver fibrosis and cancer (Tomasek *et al.*, 2002; Ingber, 2003; Paszek *et al.*, 2005; Li *et al.*, 2007; Wells and Discher, 2008; Butcher *et al.*, 2009; Hinz, 2009). In cartilage, understanding the interaction between ECM stiffness and TGFβ may elucidate mechanisms that self-promote chondrocyte differentiation in development or those that spiral out of control in OA. Therefore, using chondrocytes as an experimental model, we explore the mechanisms by which cells integrate the physical and biochemical cues provided by ECM stiffness and TGFβ, respectively.

RESULTS

Chondrocyte differentiation is tuned to an optimal ECM stiffness

To determine whether chondrocyte differentiation is sensitive to the stiffness of the extracellular microenvironment, we differentiated primary murine chondrocytes and ATDC5 chondroprogenitor cells for 2 and 7 d, respectively, on collagen II–coated polyacrylamide substrates with stiffnesses that span the range reported for articular cartilage (0.2–1.1 MPa; Table 1; Kiviranta *et al.*, 2008; Hansma *et al.*, 2009). Substrate stiffness strongly regulated expression of multiple markers of chondrocyte differentiation, including the lineage-specific transcription factor Sox9 and genes encoding the major constituents of cartilage matrix—Col2α1 and aggrecan. Specifically, in primary murine chondrocytes cultured on 0.5-MPa gel substrates, a stiffness similar to that of healthy articular cartilage, Sox9, Col2α1, and aggrecan are induced 2-, 2.5-, and 3-fold, respectively, relative to the plastic control (Figure 1A). Moreover, these genes are not induced on substrates with a stiffness greater or less than 0.5 MPa, demonstrating the specificity of stiffness-induced chondrocyte gene expression. This stiffness-specific induction was even more robust in ATDC5 cells, with Sox9, Col2α1, and aggrecan mRNA expression induced 6-, 19-, and 16-fold, respectively, on 0.5-MPa substrates relative to the plastic control (Figure 1B). These changes in chondrocyte gene expression are accompanied by a stiffness-sensitive production of proteoglycan in ATDC5 cells, as detected by Alcian blue staining, which is also maximal on the 0.5-MPa gel (Figure 1C). Therefore chondrocyte differentiation is carefully tuned to the stiffness of the extracellular matrix, such that maximal differentiation occurs on substrates that mimic the stiffness of native healthy articular cartilage.

Material	Substrate name	Stiffness (MPa)	Composition		Collagen density (μg/cm²)	Cell characterization	
			Acrylamide (% wt)	Piperazine diacrylamide (% wt)		Average cell area (μm²)	Average roundness[a]
Polyacrylamide gels	0.2 MPa	0.19 ± 0.03	30	1	1.34 ± 0.72	1062 ± 629	0.67 ± 0.16
	0.5 MPa	0.53 ± 0.03	30	2	1.81 ± 1.02	1041 ± 637	0.66 ± 0.16
	1.1 MPa	1.11 ± 0.08	30	3	2.05 ± 0.57	1137 ± 820	0.66 ± 0.17
Tissue culture plastic	Plastic	10^6	N/A	N/A	1.17 ± 0.12	1113 ± 637	0.63 ± 0.16
Articular cartilage	N/A	0.2–1					

Polyacrylamide gel substrates are referred to in this article by their average stiffness, measured previously by nanoindentation (values are from Hansma *et al.*, 2009). These values span the stiffness range reported for articular cartilage, also measured by nanoindentation (values are from Kiviranta *et al.*, 2008). Collagen density between substrates was found to be statistically indistinguishable ($p > 0.05$). ATDC5 cell morphology was also found to be statistically indistinguishable, given by average cell area and roundness.
[a]Varies from 0 to 1, where 1 = circular.

TABLE 1: Physical characteristics of experimental substrates.

Potent chondroinductive synergy between ECM stiffness and TGFβ

The cellular microenvironment is rich in both biochemical and physical cues that can potently regulate differentiation and cell behavior. Therefore we evaluated the effect of substrate stiffness on chondrogenic differentiation in the presence or absence of TGFβ, a potent biochemical agonist of chondrocyte differentiation (Blaney Davidson *et al.*, 2007; Derynck *et al.*, 2008). TGFβ induces the expression of Col2α1 and aggrecan in differentiating ATDC5 cells grown for 7 d on plastic substrates (Figure 2, A–C). Interestingly, ATDC5 cells exhibit an equivalent chondroinductive response to a 0.5-MPa substrate as to TGFβ (Figure 2, A–C). Even these responses, however, pale in comparison to the strong synergistic induction of Sox9, Col2α1, and aggrecan expression (9-, 140-, and 70-fold, respectively) in TGFβ-treated ATDC5 cells differentiated for 7 d on 0.5-MPa substrates (Figure 2, A–C). This powerful chondroinductive synergy demonstrates that the cellular response to TGFβ is highly dependent on the physical microenvironment.

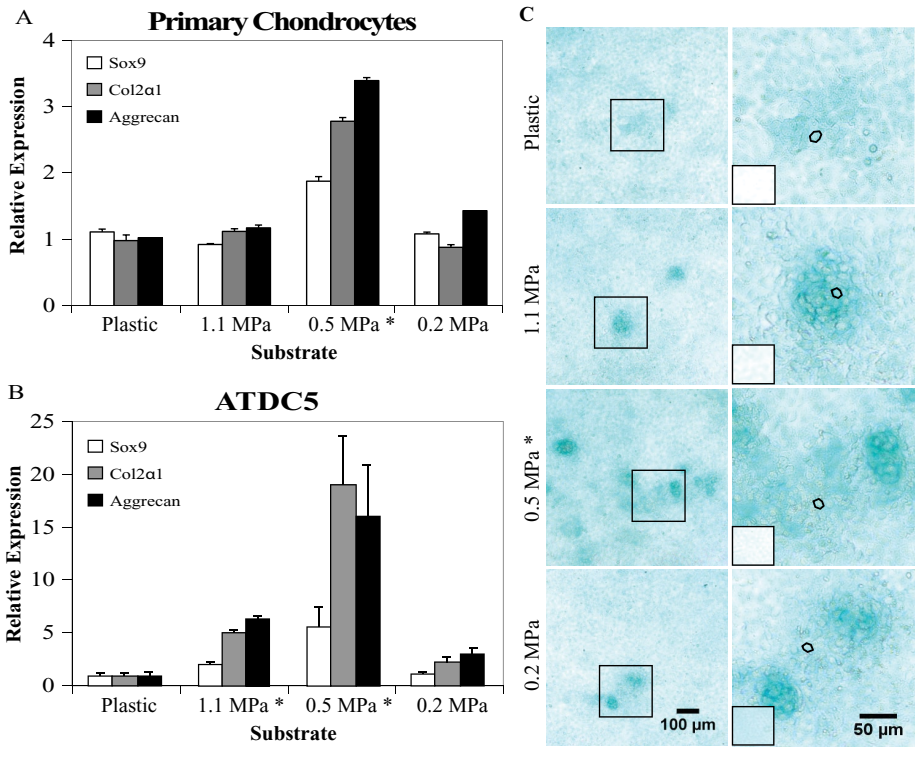

FIGURE 1: Chondrocyte differentiation is stiffness sensitive. Primary murine chondrocytes (A) and ATDC5 cells (B) cultured in differentiation media on plastic or polyacrylamide gels of the indicated stiffness demonstrate the greatest increase in Sox9, Col2α1, and aggrecan gene expression on 0.5-MPa substrates, similar to the stiffness of articular cartilage. (C) Alcian blue staining of proteoglycan production, a functional measure of chondrocyte differentiation, reveals a significant 3.1-fold increase in stained area for ATDC5 cells grown on 0.5-MPa substrates relative to cells grown on plastic. Right, high-magnification images of regions outlined on the left. Staining localizes to regions between cells (a single cell perimeter is marked by a dotted line). The small box to the bottom left of each image shows background Alcian blue staining of control cell-free substrates. *$p < 0.05$.

Mechanosensitive chondroinduction is mediated by ROCK signaling

The potent chondroinductive response of ATDC5 cells to substrate stiffness provides a tractable in vitro model system to explore the mechanisms of stiffness-induced chondrocyte differentiation. Cells respond to substrate stiffness by increasing internal cellular tension through stress fiber formation and cell spreading (Discher *et al.*, 2005). Although ATDC5 morphology and cell spread area do not vary significantly across the substrate stiffnesses tested (Table 1), stress fiber formation in ATDC5 cells also increases with substrate stiffness (Figure 3B). This suggests that induction of chondrocyte differentiation on 0.5-MPa substrates is mediated through internal cell tension. As key components of the cellular mechanosensory apparatus, Rho and ROCK participate in stiffness sensing in

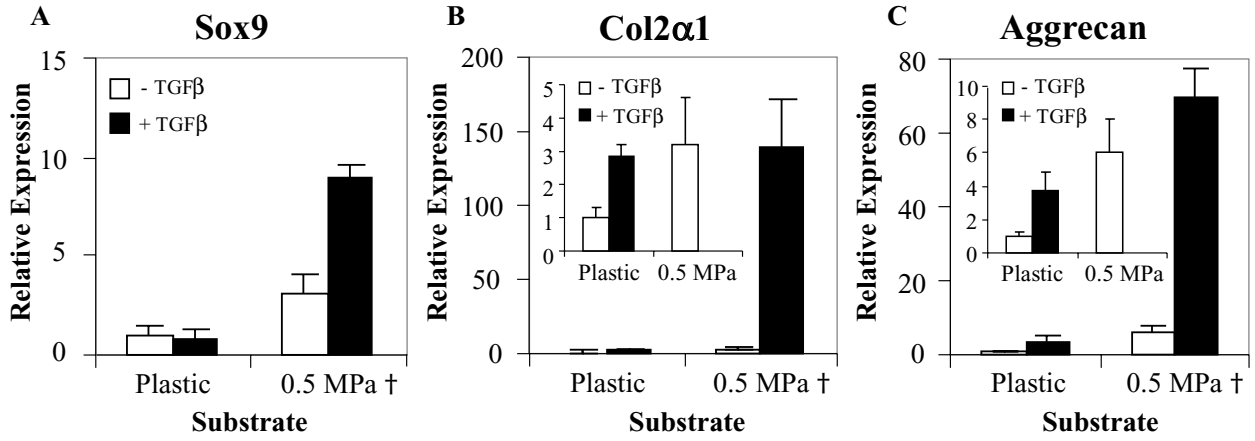

FIGURE 2: Substrate stiffness and TGFβ synergize to induce chondrogenic differentiation. Sox9 (A), Col2α1 (B), and aggrecan (C) mRNA expression is greatly induced by TGFβ (5 ng/ml) in ATDC5 cells differentiated for 7 d on 0.5-MPa substrates relative to cells grown on plastic or in the absence of TGFβ. $p < 0.01$.

part through stress fiber formation (Amano *et al.*, 1997; Maekawa *et al.*, 1999). ROCK activity increases with substrate stiffness, such that cells cultured on stiffer substrates (i.e., plastic) generate higher ROCK activity than cells cultured on more compliant substrates (Huang and Ingber, 2005). To determine whether the chondroinductive effect of substrate stiffness occurs through these established mechanisms, we treated primary murine chondrocytes and ATDC5 cells with the ROCK inhibitor Y27632. On plastic, inhibition of ROCK enhances the expression of Col2α1 mRNA after 48 h of culture (Figure 3C). However, on a substrate that mimics the stiffness of articular cartilage, ROCK inhibition completely represses the induction of Col2α1. Similar results are seen in Sox9 and aggrecan expression. This observation confirms the key role for ROCK in the ability of chondrocytes to sense and respond to ECM stiffness.

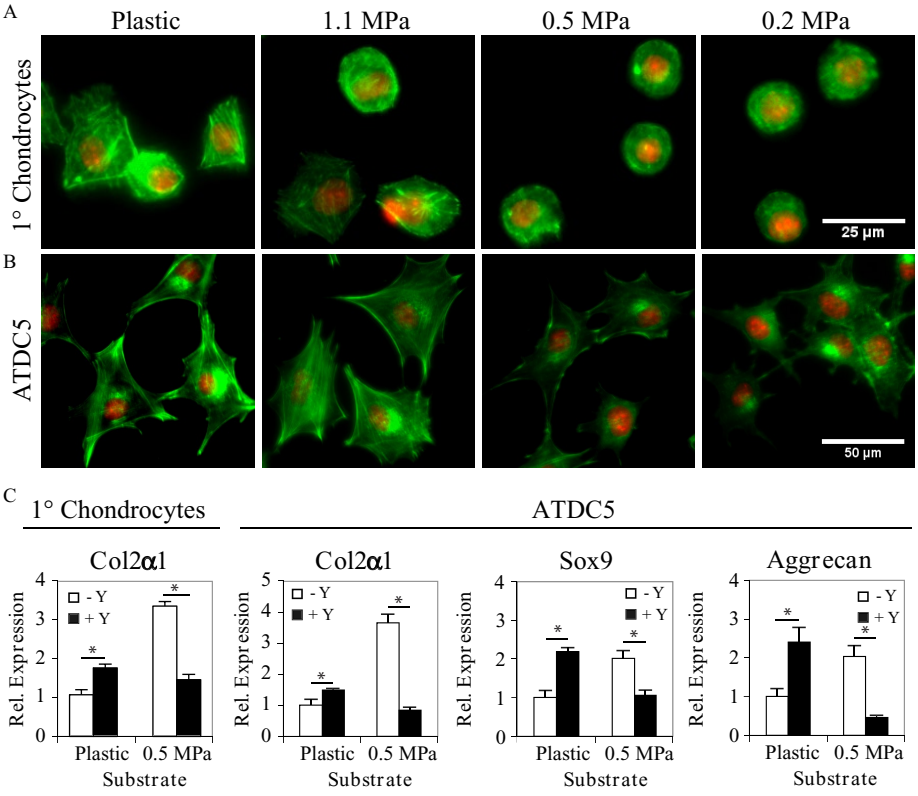

FIGURE 3: Mechanosensitive chondroinduction is mediated by ROCK signaling. Stress fibers, visualized by rhodamine phalloidin (green), are visible in primary chondrocytes (A) and ATDC5 cells (B) with greater frequency and intensity on substrates with stiffnesses of 1.1 MPa or greater. Nuclei are stained with DAPI (red). (C) ROCK inhibition with Y27632 (Y, 10 μM) induces Col2α1 in primary chondrocytes and ATDC5 cells differentiated for 24 h on plastic but represses induction in cells differentiated on 0.5-MPa substrates. Similar results are seen for Sox9 and aggrecan expression. *$p < 0.05$.

Mechanosensitive TGFβ1 expression promotes chondrogenic differentiation

The effect of ECM stiffness on primary murine chondrocytes and ATDC5 gene expression is apparent within 48 h, when Col2α1 mRNA levels are increased in cells grown on 0.5-MPa substrates relative to those grown on plastic (Figure 3C). At this time, TGFβ1 mRNA expression is increased threefold in primary murine chondrocytes and ATDC5 cells cultured on a 0.5-MPa substrate, a finding confirmed by enzyme-linked immunosorbent assay (ELISA) analysis of TGFβ1 protein levels in ATDC5-conditioned media (Figure 4, A–C). Although others have shown that TGFβ1 mRNA and protein expression are regulated in response to exogenous physical stimuli (Streuli *et al.*, 1993; Sakai *et al.*, 1998; Li *et al.*, 2010b), to our knowledge this is the first report that substrate stiffness can regulate expression of a TGFβ ligand.

We assessed the stiffness specificity of the induction of TGFβ1 mRNA and protein. Levels of both TGFβ1 mRNA and protein increased with substrate compliance (Figure 4C and unpublished data). The ROCK inhibitor Y27632 increased

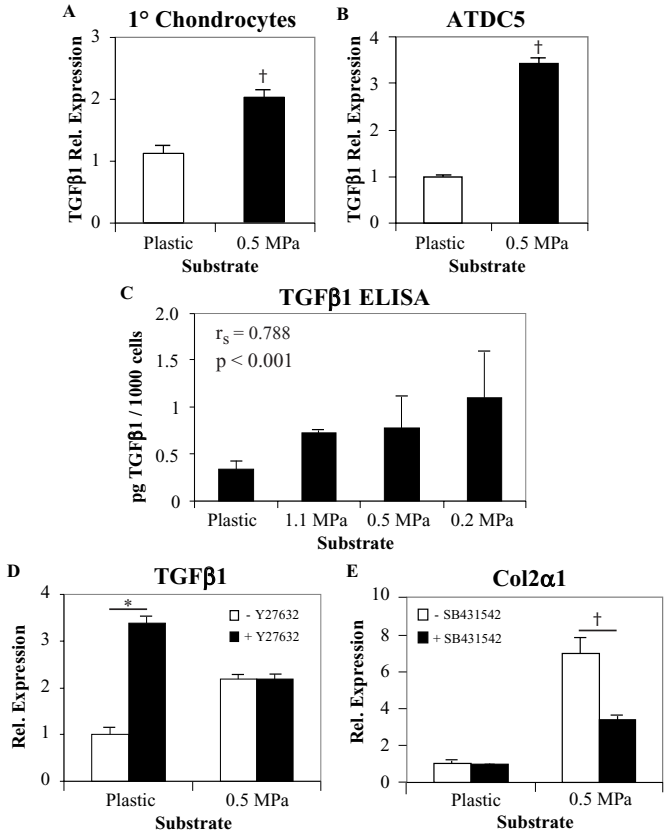

FIGURE 4: Mechanosensitive, ROCK-dependent induction of TGFβ1 is required for chondroinduction. Within 48 h, TGFβ1 mRNA is induced in primary chondrocytes (A) and ATDC5 cells (B) in a stiffness-dependent manner. (C) TGFβ1 protein produced by ATDC5 cells, as assessed in media by an ELISA, increases with decreasing substrate stiffness. (D) The expression of TGFβ1 mRNA in ATDC5 cells is increased by ROCK inhibition with Y27632 (10 μM) on plastic but is unaffected on 0.5-MPa substrates. (E) Induction of Col2α1 mRNA in ATDC5 cells cultured on a 0.5-MPa gel is impaired by 24-h exposure to SB431542 (5 μM), a chemical antagonist of the TGFβ type I receptor. *$p < 0.05$, $p < 0.01$.

TGFβ1 expression in cells cultured on plastic but had no effect on cells grown on 0.5-MPa substrates (Figure 4D), suggesting that TGFβ1 expression is induced on compliant substrates due to reduced ROCK activity. This stiffness-dependent pattern of TGFβ1 gene expression is distinct from that of chondrocyte differentiation genes, which is induced specifically on 0.5-MPa substrates.

To determine whether the stiffness-sensitive increase in autocrine TGFβ1 expression is required for the chondroinductive effects of the 0.5 MPa substrate, we treated ATDC5 cells with a TβRI inhibitor (SB431542) that acts downstream of the TGFβ1 ligand. Although baseline levels of Col2α1 in ATDC5 cells cultured on plastic were not sensitive to the inhibitor, the induction of Col2α1 on 0.5-MPa substrates was diminished by the TβRI inhibitor (Figure 4E). Therefore the chondroinductive response to substrate stiffness requires a mechanosensitive induction of autocrine TGFβ1. However, this mechanism alone does not fully explain why chondrocyte gene expression is optimal on 0.5-MPa substrates since, on more compliant substrates, TGF-β1 is induced but chondrogenic genes are not.

Mechanosensitive regulation of Smad3 stability, phosphorylation, and translocation

We next examined the effect of substrate stiffness on Smad3, a key effector of TGFβ signaling that is phosphorylated upon ligand activation of the TGFβ receptor complex (Wrana, 2000). Although no significant stiffness-dependent changes in Smad3 mRNA levels were detected (Supplemental Figure S1), Smad3 protein levels were consistently elevated in ATDC5 cells grown on 0.5-MPa substrates (Figure 5A). Furthermore, even in the absence of exogenously added TGFβ, Smad3 phosphorylation on the C-terminal SSXS domain was increased on 0.5-MPa substrates relative to that observed on either stiffer or more compliant substrates (Figure 5A). In ATDC5 chondroprogenitor cells, this stiffness-specific increase in Smad3 phosphorylation mirrored the specific increase in chondrogenic gene expression on 0.5-MPa substrates (Figure 1A). From this result, it appears that on overly compliant substrates, even in the presence of increased autocrine TGFβ1 expression (Figure 4C), the lack of chondroinduction might be due to other mechanisms, such as those limiting ligand-mediated activation of the downstream effector Smad3.

Consistent with its increased phosphorylation, Smad3 preferentially localizes to the nucleus of primary murine chondrocytes and ATDC5 cells grown on 0.5-MPa substrates. Nuclear Smad3 localization is as frequent in cells grown on 0.5-MPa substrates in the absence of exogenously added TGFβ as in TGFβ-treated cells grown on plastic (Figure 5, B and C). To determine whether this stiffness-dependent increase in nuclear Smad3 is sufficient to induce transactivation, we assessed the effect of substrate stiffness on the activation of a classic Smad3-responsive promoter-reporter construct, SBE-luciferase (Figure 5D). Transactivation of SBE-luciferase is increased in ATDC5 cells grown on 0.5-MPa substrates relative to those grown on plastic. Together these findings suggest that the TGFβ pathway exhibits stiffness-sensitive regulation at multiple levels, including posttranscriptional control of Smad3 levels, phosphorylation, localization, and transactivation, all of which are maximal in chondroprogenitor cells grown on 0.5-MPa substrates that mimic the stiffness of healthy articular cartilage.

Synergistic response to TGFβ and substrate stiffness requires p38 MAPK but not Smad3

The potent synergistic response of ATDC5 cells to substrate stiffness and exogenously added TGFβ seen in Figure 2 provides an ideal model system for the study of the molecular mechanisms by which cells integrate signaling from physical and biochemical cues. Therefore we sought to determine which of the downstream effectors of TGFβ participate in the chondroinductive synergy between exogenously added TGFβ and substrate stiffness. As in Figure 5A, Smad3 and phospho-Smad3 levels are increased in ATDC5 cells grown on 0.5-MPa substrates relative to those grown on plastic (Figure 6A). The addition of TGFβ increased the level of Smad3 phosphorylation to a similar level regardless of substrate stiffness, suggesting that factors in addition to elevated TGFβ1, as in Figure 4C, are required for synergy. In Smad3 short hairpin RNA (shRNA)–expressing cells (Figure 6B), induction of Col2α1 by stiffness alone is impaired (Figure 6C). However, even with a 70% reduction in Smad3 levels, Col2α1 expression in ATDC5 cells is still synergistically induced by exogenously added TGFβ in ATDC5 cells grown on a 0.5-MPa substrate (Figure 6C). In these conditions, Smad2 mRNA expression is not increased to compensate for the decreased expression of Smad3 (unpublished data). Synergy was also unaffected in $Smad3^{fl/fl}$ primary articular chondrocytes infected with CRE adenovirus (unpublished data). Therefore the cooperative induction of

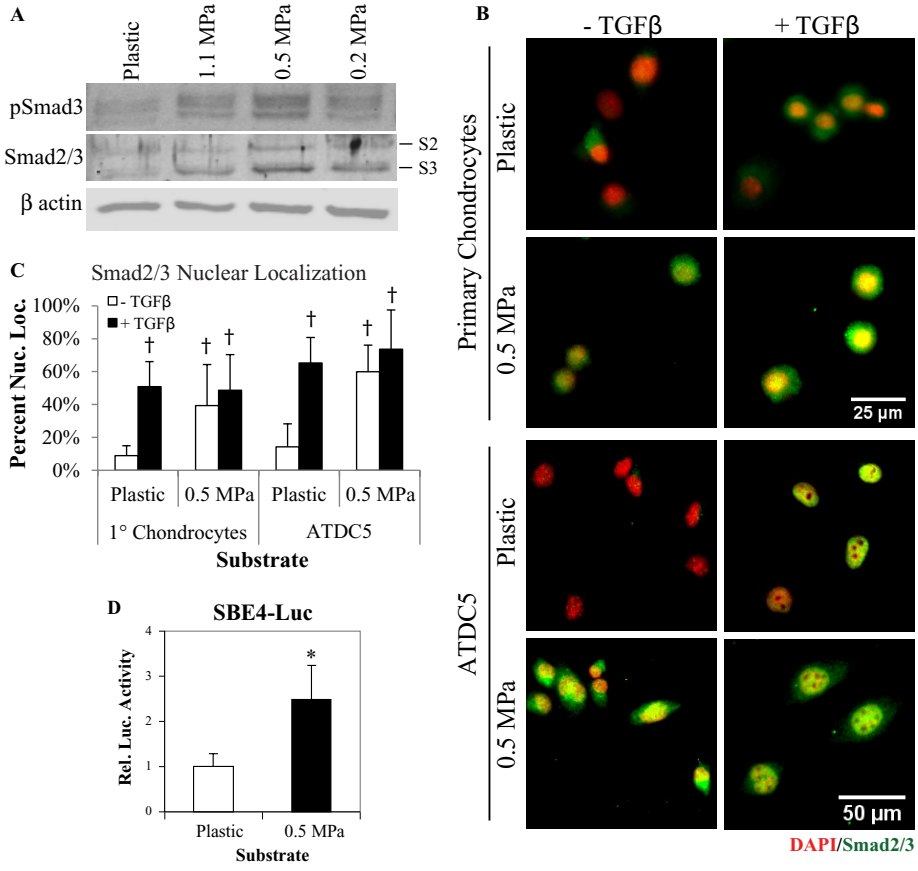

FIGURE 5: Smad3 phosphorylation, localization, and transcriptional activity are sensitive to ECM stiffness. (A) Western analysis of whole-cell lysates from ATDC5 cells cultured as indicated for 24 h reveals that C-terminal Smad3 phosphorylation (top) and total protein (middle) are increased specifically on a 0.5-MPa substrate, whereas β-actin levels (bottom) remain unchanged. (B) Immunofluorescence microscopy allows visualization of stiffness and TGFβ-sensitive Smad2/3 localization (green) relative to DAPI-stained nuclei (red). (C) Relative to cells grown on plastic, a greater percentage of primary chondrocytes and ATDC5 cells have nuclear Smad2/3 when grown on 0.5-MPa substrates, particularly in the absence added TGFβ. (D) In transiently transfected ATDC5 cells grown for 48 h on 0.5-MPa substrates, the activity of the TGFβ-responsive SBE-luciferase promoter reporter construct is increased relative to cells grown on plastic. Luciferase activity is normalized to expression of β-galactosidase from a cotransfected control construct. *$p < 0.05$, $p < 0.01$.

chondrogenic gene expression between TGFβ and 0.5-MPa substrates occurs through a Smad3-independent pathway.

As a first step in examining the role of another well-known target of TGFβ signaling in the synergistic induction of Col2α1, we evaluated the effect of substrate stiffness and TGFβ on p38 MAPK phosphorylation. TGFβ rapidly activates the p38 pathway through the MAPK kinase kinase TAK1 activation of MKK3/6 (Moriguchi *et al.*, 1996; Derynck and Zhang, 2003). Phospho-p38 was increased on 0.5-MPa substrates relative to plastic (Figure 6D). TGFβ-induced p38 phosphorylation in ATDC5 cells grown on plastic and on 0.5-MPa substrates but not in a synergistic manner. Nonetheless, p38 is critically involved in synergy since the p38 inhibitor SB203580 strongly repressed the Col2α1 induction in response to exogenously added TGFβ in ATDC5 cells grown on a 0.5-MPa substrate. Whereas the p38 inhibitor caused a 2.5-fold repression of Col2α1 expression on 0.5-MPa gels alone, it was responsible for a 5-fold repression of the synergistic response (Figure 6E). This suggests that p38 participates in the chondroinductive effects of substrate stiffness and is essential for the integration of physical and biochemical cues that robustly promotes chondrogenic differentiation on substrates that mimic the stiffness of healthy articular cartilage.

DISCUSSION

We elucidated mechanisms by which physical cues provided by a discrete ECM stiffness specifically increase the efficiency of chondrocyte differentiation by coordinated multilevel regulation of the TGFβ pathway (Figure 7). A cartilage-like substrate stiffness both enhances chondrocyte gene expression and primes cells for a robust response to the chondroinductive biochemical cue TGFβ. In this way, the convergence of chondroinductive physical and biochemical cues drives a more potent response than either cue alone, thereby establishing a microenvironment that the cells interpret as ideal for chondrocyte differentiation. Through ROCK signaling, ECM stiffness regulates chondrocyte differentiation by promoting autocrine TGFβ1 expression on compliant substrates. Stiffness-sensitive chondrocyte differentiation requires Smad3, the phosphorylation of which is maximal on the same discrete stiffness that optimally induces chondrocyte gene expression. In addition to regulating TGFβ ligand expression and Smad3 phosphorylation, localization, and transactivation, cells respond to exogenously added TGFβ on a cartilage-like stiffness with a p38 MAPK-dependent synergistic induction of chondrocyte gene expression. Therefore, by ECM stiffness-dependent calibration of the TGFβ pathway, chondrocytes integrate physical and biochemical cues to efficiently promote cell differentiation.

We find that the cellular response to ECM stiffness targets the TGFβ pathway at several hierarchical levels. Cellular mechanosensing of ECM stiffness requires the development of cytoskeletal tension and the activation of Rho/ROCK (Miranti and Brugge, 2002; Assoian and Klein, 2008; Geiger *et al.*, 2009; Kanchanawong *et al.*, 2010), a pathway previously implicated in chondrocyte differentiation (Wang *et al.*, 2004; Woods and Beier, 2006). The role of Rho/ROCK signaling in chondrogenesis is complex, such that the effect of ROCK inhibition on chondrogenic differentiation is influenced by the cell type and the dimensionality of culture, among other factors (Clancy *et al.*, 1997; Nofal and Knudson, 2002; Woods *et al.*, 2005; Woods and Beier, 2006; Kumar and Lassar, 2009). Like Woods *et al.* (2005), we find that chondrocyte differentiation is ROCK dependent, such that inhibition of ROCK enhances differentiation of cells grown on plastic but inhibits differentiation in cells grown in more compliant conditions (Figure 3C). Our results suggest that there is an optimal level of ROCK activity on 0.5-MPa substrates that activates chondroinduction, in part, through the induction of TGFβ1 expression on compliant substrates. To our knowledge, this is the first report of a component of the TGFβ pathway regulated in a stiffness-dependent manner. Although the transcriptional mechanisms by which ECM stiffness regulates TGFβ1 expression remain to be explored, other

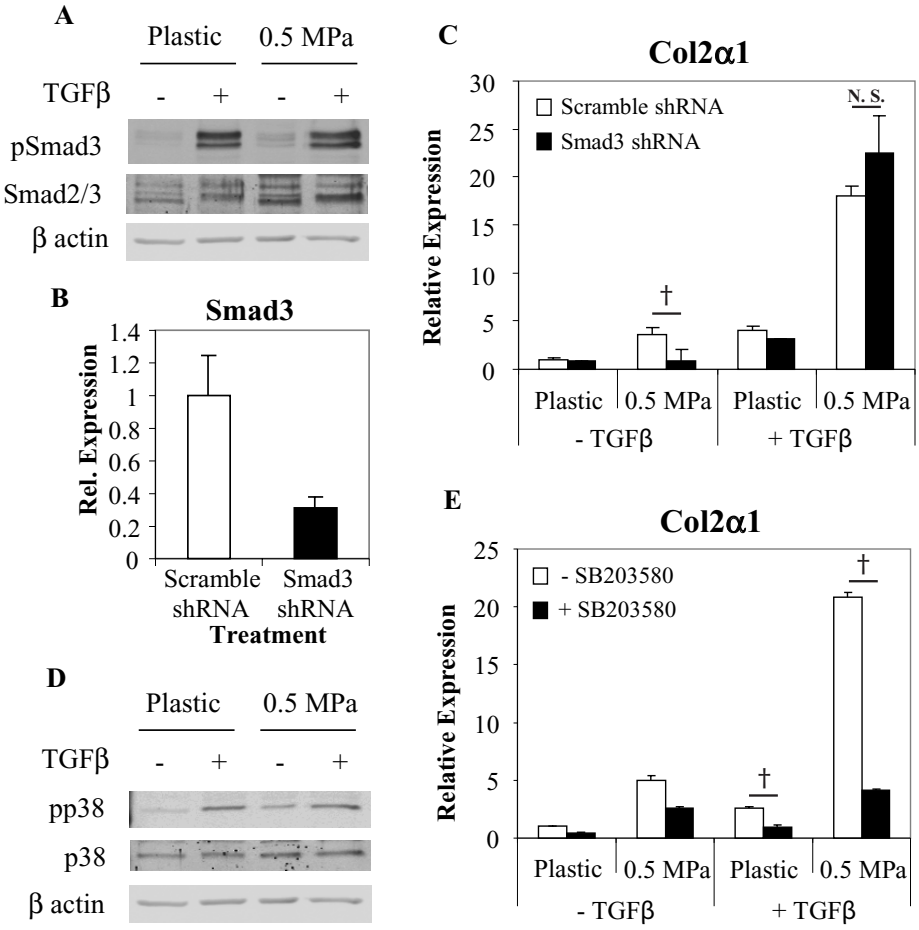

FIGURE 6: Synergy between TGFβ and ECM stiffness requires p38 MAPK but not Smad3. (A) Western analysis reveals no substrate stiffness-dependent effect on TGFβ-inducible Smad3 phosphorylation. (B) Smad3 shRNA treatment achieves 70% reduction of Smad3 mRNA relative to ATDC5 cells expressing a scrambled shRNA. (C) shSmad3 impairs the stiffness-sensitive induction of Col2α1 mRNA but not the synergistic induction of Col2α1 by TGFβ (5 ng/ml, 24 h) and a 0.5-MPa substrate. (D) Western analysis of phospho-p38 and p38 total protein reveals increased p38 phosphorylation in ATDCs cultured for 24 h on a 0.5-MPa substrate or in the presence of TGFβ (5 ng/ml, 45 min). (E) Synergistic induction of Col2α1 mRNA by a 0.5-MPa substrate and TGFβ is greatly reduced upon inhibition of p38 activity by SB203580 (10 μM) before a 1-h TGFβ treatment. $p < 0.01$.

physical stimuli have been shown to regulate TGFβ1 expression and activity. TGFβ1 mRNA expression is induced by shear fluid flow, in vitro compressive loading, or culture on floating substrates (Streuli *et al.*, 1993; Sakai *et al.*, 1998; Li *et al.*, 2010b). Myocyte stretch induces the release of activated TGFβ1 from the latency-associated peptide on stiff substrates (Wells and Discher, 2008; Hinz, 2009). Future studies will test the hypothesis that this combination of regulatory mechanisms—ECM stiffness-sensitive induction of TGFβ1 transcription on compliant substrates and posttranslational TGFβ1 activation on stiff substrates—contributes to the potent stiffness-specific chondroinduction in ATDC5 cells and primary chondrocytes (0.5 MPa).

This hierarchical regulation continues inside the cell, where ECM stiffness targets the key TGFβ effector Smad3. ATDC5 cells grown on the chondroinductive 0.5-MPa substrates exhibit a specific increase in Smad3 phosphorylation. Phosphorylated Smad3 translocates to the nucleus, where it can bind to Sox9 and enhance CBP recruitment to the Col2α1 promoter, where they cooperatively induce Col2α1 transcription (Furumatsu *et al.*, 2005). We found that the stiffness-specific phosphorylation and nuclear localization of Smad3 correlates with and is required for the increased Col2α1 expression on 0.5-MPa substrates. Although several mechanisms may contribute to these observations, our data strongly suggest that autocrine TGFβ1 activity is significantly responsible for the stiffness-specific increase in Smad3 phosphorylation and the resulting induction of Col2α1. Treatment with either a TGFβ receptor inhibitor or shSmad3 completely ablates the induction of Col2α1 gene expression on 0.5-MPa substrates. Although collagen II has also been shown to induce phosphorylation of Smad2/3 in the absence of exogenous TGFβ (Garamszegi *et al.*, 2010), collagen II density did not vary greatly with substrate stiffness in our experiments.

Numerous links between Smad signaling and effectors of the mechanosensing pathway have been identified. Cytoskeletal tension, generated by either ECM stiffness or cell spreading, is sufficient to control the localization of YAP/TAZ (Dupont *et al.*, 2011), transcriptional coregulators that can direct nuclear localization of Smad2/3 (Varelas *et al.*, 2008). More recently, Wang *et al.* (2012) showed that BMP-inducible nuclear translocation of Smad1/5/8 requires sufficient ROCK-dependent cytoskeletal tension. ROCK can also enhance the activity of both Smad3 and Sox9 by phosphorylation of the Smad3 linker region or Sox9 on serine 181 (Kamaraju and Roberts, 2005; Haudenschild *et al.*, 2010). Although the role of ROCK-inducible Sox9 phosphorylation in the chondroinductive synergy between ECM stiffness and TGFβ remains unclear, this synergistic response does require p38 MAPK and functions even with very little Smad3. This is consistent with prior studies showing that TAK1, the upstream activator of p38 MAPK, regulates collagen II synthesis in chondrocytes independently of Smad3 signaling (Qiao *et al.*, 2005). ECM stiffness may also cause differential utilization of downstream TGFβ receptors or effectors (Blaney Davidson *et al.*, 2009; van der Kraan *et al.*, 2009), or it may prime chromatin for a more potent TGFβ-inducible transactivation (Mullen *et al.* 2011), mechanisms shown to calibrate the cellular response to TGFβ in osteoarthritic chondrocytes or in differentiating stem cells, respectively. Additional studies are needed to further investigate the synergistic response of chondrocytes to ECM stiffness and TGFβ, work that will elucidate new mechanisms by which cells integrate physical and biochemical cues to refine and coordinate cell behavior, a paradigm that has relevance for cartilage and many other tissues. Nonetheless, the present work illustrates that cells respond to a chondroinductive physical cue (a cartilage-like substrate stiffness) by strategically targeting the activity of a powerful chondroinductive biochemical pathway (TGFβ) at multiple hierarchical levels.

The range of stiffnesses present in cartilage varies spatially and temporally, such that each may have unique instructive roles. Consistent with the stiffness of adult articular cartilage, precommitted

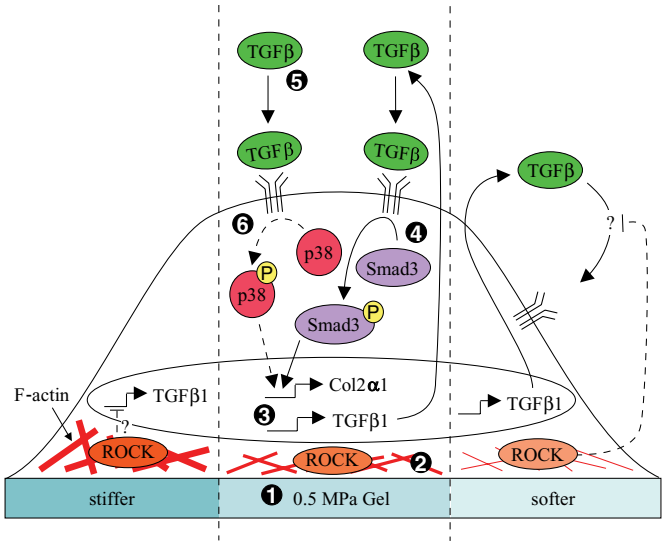

FIGURE 7: Schematic of the mechanism of chondrocyte integration of cues provided by ECM stiffness and TGFβ. 1) Chondrocyte differentiation is specifically induced on 0.5-MPa substrates. 2) This response is mediated through the ROCK pathway. 3) Autocrine TGFβ1 expression is required for chondroinduction, the expression of which is inhibited on stiffer substrates through a ROCK-dependent mechanism. 4) Whereas Smad3 phosphorylation and nuclear localization are increased on 0.5-MPa substrates, softer substrates that express autocrine TGFβ fail to activate this downstream effector. 5) Exogenously added TGFβ elicits a synergistic response in combination with 0.5-MPa substrates. 6) This synergistic interaction acts through a p38-MAPK–dependent mechanism, possibly through TGFβ activation of TAK1.

chondrocytes (ATDC5 chondroprogenitors or primary chondrocytes) showed maximal chondrocyte gene expression on 0.5-MPa substrates. More compliant matrices may be more chondroinductive during lineage selection, as induction of chondrogenic gene expression in MSCs occurs on compliant 1-kPa substrates (Park *et al.*, 2011). Indeed, osteogenic differentiation in MSCs has been reported on a 25-kPa substrate, which is softer than fully mineralized bone matrix (Engler *et al.*, 2006). This relationship between ECM stiffness and chondrocyte differentiation, also observed in other species (Schuh *et al.*, 2010), may be particularly important for understanding OA, in which the degradation of cartilage ECM stiffness coincides with the loss of chondrocyte homeostasis through mechanisms that are coupled but unclear. Because TGFβ signaling through the p38 MAPK pathway is important in vitro and in vivo for chondrocyte maturation, proliferation, and survival (Seto *et al.*, 2004; Gunnell *et al.*, 2010; Li *et al.*, 2010a), our finding that p38 MAPK is important for of synergy between TGFβ and substrate stiffness suggests that coordinated signaling between biochemical and physical cues may be important for the maintenance of chondrocyte homeostasis. The ability of ECM stiffness to modulate the cellular response to TGFβ, in particular, may elucidate the differential effects of this growth factor on chondrocytes, such that it can either promote or deter this degenerative cascade in a way that is highly sensitive to the cellular microenvironment (Blaney Davidson *et al.*, 2007).

Within and beyond cartilage, the interaction between TGFβ and ECM stiffness may form a feedback loop to promote and maintain cellular homeostasis and ECM composition. TGFβ plays a primary role in regulating ECM composition and stiffness in several tissues, including bone, dentin, and skin (Balooch *et al.*, 2005; Arany *et al.*, 2006; Saeki *et al.*, 2007; Chang *et al.*, 2010). Therefore disruption of TGFβ signaling impairs ECM stiffness, and, as we show here, disruption of ECM stiffness alters the level of and cellular response to TGFβ signaling. Indeed, in several other diseases, including breast cancer and liver fibrosis, the pathological phenotype is accompanied and perpetuated by nonphysiologic stiffnesses and abnormal TGFβ signaling (Tomasek *et al.*, 2002; Ingber, 2003; Paszek *et al.*, 2005; Li *et al.*, 2007; Wells and Discher, 2008; Butcher *et al.*, 2009; Hinz, 2009). A deeper understanding of the interactions between physical and biochemical cues, particularly the mechanisms by which cells integrate cues provided by ECM stiffness and TGFβ, may elucidate mechanisms of disease and reveal novel therapeutic targets.

MATERIALS AND METHODS

Gel substrate preparation

The elastic modulus of polyacrylamide gel substrates was controlled by varying the concentration of the cross-linker, piperazine diacrylamide (Bio-Rad, Hercules, CA 161-0202), from 1–3% (wt/vol), while maintaining a constant 30% (wt/vol) concentration of the monomer, acrylamide (161, 0140; Bio-Rad), in a solution of 0.01 M 4-(2-hydroxyethyl)-1-piperazineethanesulfonic acid (HEPES) buffer. Polymerization was initiated by 10% (wt/vol) ammonium persulfate (APS) added at a 1:200 dilution and enhanced by TEMED (161-0801; Bio-Rad) added at a 1:2000 dilution. Before addition of APS, the acrylamide mixture was vortexed and degassed for 1 h. Gels were polymerized in a 1-mm-thick vertical glass mold and then stored in phosphate-buffered saline (PBS) at 4°C. The gels prepared in this study ranged in stiffness from 0.2 to 1.1 MPa, which spanned the range of articular cartilage (Table 1).

Cell attachment was facilitated by covalently attaching collagen II (C9301; Sigma-Aldrich, St. Louis, MO) to the polyacrylamide gel as described previously (Reinhart-King *et al.*, 2005), modified to use acrylic acid *n*-hydroxysuccinimide ester (N2; A8060; Sigma-Aldrich). A 1.8% (wt/vol) solution of N2 in 50% ethanol was diluted 1:6 into a solution containing 0.01% (wt/vol) bisacrylamide (161-0142; Bio-Rad), 0.17% (wt/vol) Irgacure 2959 (55047962; BASF, Florham Park, NJ), and 0.05 M HEPES NaOH (pH 6). Polyacrylamide gel slabs were cut into 3-cm-diameter disks with a stainless steel biscuit cutter. The gel disks were covered with 200 µl of N2 solution and sandwiched horizontally between two large glass slides before exposure to UV light (306 nm) for 10 min, followed by rinsing with PBS. Collagen II was dissolved in 0.1 M acetic acid at a concentration of 1 mg/ml and then diluted 1:100 in 1 M HEPES (pH 8). Each gel was incubated with 1 ml of the collagen II solution at 4°C overnight in ultralow-attachment six-well plates (3471; Costar, Cambridge, MA) with constant agitation. Gel substrates were washed once more with PBS and allowed to equilibrate for at least 3 h in media (50/50 DMEM/F12) at 4°C before seeding of cells. Plastic controls were coated with 1 mg/ml collagen II in acetic acid diluted 1:100 in sterile water for a minimum of 4 h at room temperature. The remaining solution was then removed, and the plates were left to dry overnight at 4°C, followed by a rinse with PBS before seeding cells.

To determine the collagen II ligand density for each substrate, we performed an indirect ELISA on collagen II–coated gels and plastic using a primary mouse antibody raised against collagen II (C11C1; Development Studies Hybridoma Bank, University of Iowa, Iowa City, IA) and an Alexa Fluor 488 goat anti-mouse secondary (A11029; Invitrogen, Carlsbad, CA). A dilution series of collagen II coated on plastic, prepared as for the experimental conditions, served as a standard curve. Fluorescence was measured in a SpectraMax M5 plate reader (Molecular Devices, Sunnyvale, CA) and normalized to the standard curve. The given values are averages of four replicates.

Collagen densities between substrates were found to be statistically indistinguishable through analysis of variance (ANOVA; Table 1).

Cell culture

A majority of the studies used ATDC5 cells, a murine chondroprogenitor cell line (RCB0565; RIKEN, Wako, Japan). Growth media for ATDC5 cells consisted of 50/50 DMEM/F12 with 5% FBS and was also used for experiments lasting <48 h. Experiments lasting 7 d were performed in differentiation media consisting of growth media supplemented with 10 µg/ml insulin (I9278; Sigma-Aldrich), 10 µg/ml transferrin (02-0124SA; Life Technologies, Carlsbad, CA), 3×10^{-8} M sodium selenite (S5261; Sigma-Aldrich), and 1% penicillin/streptomycin. For Alcian blue staining, differentiation medium was supplemented with 25 µg/ml of ascorbic acid (A8960; Sigma-Aldrich).

Primary chondrocytes were isolated from 5-d old-mice, as described previously (Thirion and Berenbaum, 2004). Briefly, cartilage from the femoral heads, tibial plateaus, and femoral condyles was removed, cleaned of all extraneous tissue through a serial digestion in cell culture medium consisting of DMEM supplemented with 2 mM L-glutamine and 0.5% penicillin/streptomycin, with 3 mg/ml collagenase D (11 088 858 001; Roche, Indianapolis, IN) twice for 45 min, and finally overnight in cell culture medium with 0.5 mg/ml collagenase D. The remaining cell suspension was passed through a sterile 48-µm mesh and then plated directly onto experimental substrates at a density similar to that of ATDC5 cells (6000 cells/cm^2). Differentiation experiments were performed in media consisting of 50/50 DMEM/F12 supplemented with 10% FBS, 0.5% penicillin/streptomycin, 10 µg/ml insulin, 10 µg/ml transferrin, and 3×10^{-8} M sodium selenite. TGFβ3 (100-36E; Peprotech, Rocky Hill, NJ) was used at 5 ng/ml. Cells were treated as indicated with the ROCKI inhibitor Y27632 (Y0503; 10 µM; Sigma-Aldrich), the TGFβ receptor type I kinase inhibitor SB431542 (S4317; 5 µM; Sigma-Aldrich), and the p38 inhibitor SB203580 (559389; 10 µM; Calbiochem, La Jolla, CA).

Cell characterization

Images of ATDC5s attached to each gel substrate and plastic were taken with a Zeiss Axiovert 40CFL microscope (Zeiss, Jena, Germany) 24 h after seeding. Using ImageJ (National Institutes of Health, Bethesda, MD), the outline of each cell was drawn and analyzed for cell area and roundness ($4 \times$ cell area/$\pi \times$ major axis^2). Each image contained ~100 cells. Cell confluency in each image was calculated to be <35%. Average roundness and cell area were calculated for each image and found to be statistically indistinguishable through ANOVA. Values given in Table 1 are the averages and standard deviations for all cells analyzed across three biological replicates for each substrate.

Quantitative PCR

RNA was isolated using RNeasy column purification (74104; Qiagen, Valencia, CA). RNeasy lysis buffer was added to both gel and plastic conditions, and RNA was isolated according to manufacturer's instructions, including an on-column DNase treatment. The concentration and purity of RNA were determined using a NanoDrop ND-1000 Spectrophotometer (Thermo Scientific, Waltham, MA). Approximately 1 µg of RNA was converted to cDNA in a reverse transcription reaction using the iScript cDNA Synthesis Kit (Bio-Rad, 170-8891). Quantitative PCR analysis of each sample was performed in a C1000 Thermal Cycler with CFX96 Real-Time System (Bio-Rad). Forward and reverse intron-spanning primers (Table 2) and iQ SYBR Green Supermix (170-8882; Bio-Rad) were used to amplify each cDNA of interest. Each sample was run in duplicate, and all results were normalized to the housekeeping gene 18S or L19. Fold changes in gene expression were calculated using the delta-delta *Ct* method (Livak and Schmittgen, 2001). Figures show the mean and SD for two technical replicates in a representative experiment, each of which was repeated independently at least three times. For statistical analysis, average expression and SE of the mean were calculated for each condition from multiple biological replicates, each of which is an average of two technical replicates. ANOVA followed by Student Newman–Keuls test was used to evaluate statistical significance.

Gene		Sequence
Sox9	Forward	TCGCCTTCCCCGGGTTTAGAGC
	Reverse	GGCGGCGGGCACTTAGCAGA
Col2α1	Forward	ACGAAGCGGCTGGCAACCTCA
	Reverse	CCCTCGGCCCTCATCTCTACATCA
Aggrecan	Forward	GTGAGGACCTGGTAGTGCGAGTGA
	Reverse	GAGCCTGGGCGATAGTGGAATATA
TGFβ1	Forward	AGCCCGAAGCGGACTACTAT
	Reverse	TCCCGAATGTCTGACGTATTG
Smad3	Forward	ACCAAGTGCATTACCATCC
	Reverse	CAGTAGATAACGTGAGGGAGCCC
L19	Forward	ACGGCTTGCTGCCTTCGCAT
	Reverse	AGGAACCTTCTCTCGTCTTCCGGG
18S	Forward	GCGGCTTGGTGACTCTAGATA
	Reverse	GAATCGAACCCTGATTCCC

TABLE 2: Primers for SYBR Green detection of mouse sequences by quantitative reverse transcription-PCR analysis.

Alcian blue assay

ATDC5 cells cultured on plastic and gel substrates for 7 d were analyzed for proteoglycan production using an Alcian blue assay. Collagen II–coated plastic and gel substrates without seeded ATDC5s were used as negative controls. All substrates were rinsed with cold PBS, fixed for 30 min in 4% Formalin, rinsed with deionized water, equilibrated in 3% glacial acetic acid for 30 min, stained with 0.1% Alcian blue dissolved in 3% glacial acetic acid (pH 2.5) for 30 min with constant agitation, and rinsed with 3% glacial acetic acid three times for 30 min each. Images show the area on each substrate with the greatest concentration of staining and are representative of three or more biological replicates. Because gel substrates interfered with the traditional spectrophotometric analysis of Alcian blue staining, quantitative analysis was performed by thresholding across all substrates to select stained regions, from which pixel area was calculated. Values reflect mean fold change in stained area relative to cells grown on plastic. ANOVA followed by the Student Newman–Keuls test was used to evaluate statistical significance.

ELISA

Media were harvested from ATDC5 cells cultured on either gel or plastic substrates for 48 h as indicated. TGFβ1 levels were analyzed using an ELISA kit (MB100B; R&D Systems, Minneapolis, MN) according to the manufacturer's instructions. The kit detects total TGFβ1 levels and does not distinguish between active and inactive ligands. All data were normalized to cell number and compared

with a blank sample containing only media. Figures represent the average and SD for three or more biological replicates. Spearman rank analysis was used to evaluate the significance of the observed trend.

Transfection and luciferase assay

For transient transfection and luciferase assays, cells were seeded into six-well dishes and transfected at ~80% confluency with a total of 1 μg of $(SBE)_4$-luc reporter plasmid (Zawel *et al.*, 1998) in 100 μl of prewarmed OptiMEM with 5 μl of FuGENE 6 Transfection Reagent (11 814 443 001; Roche). All cells were cotransfected with an equivalent amount of total DNA, including 0.5 μg of pRK5-βGal reporter construct, which constitutively expresses β-galactosidase (Feng *et al.*, 1995). The next day, the media were changed prior to commencement of the indicated experimental conditions. At the completion of the experiment, cells were washed twice with PBS and lysed using 300 μl of Reporter Lysis Buffer (E397A; Promega, Madison, WI). Lysates were cleared by centrifugation and assayed for luciferase and β-gal activity according to the manufacturers' protocols (Promega and Tropix [Bedford, MA], respectively). Luciferase is expressed relative to β-galactosidase expression to normalize for technical variability. Figures represent averages and standard deviations of three biological replicates. Student's *t* test was used to evaluate statistical significance.

Smad3 ablation

ATDC5 cells plated in T75 flasks were infected by adding media containing lentivirus constructs that express either a pLKO.1 puro Smad3 shRNA (NM_016769.2-1430s1c1; Sigma-Aldrich) or a nontargeting shRNA sequence (SHC002; Sigma-Aldrich), which was used as a negative control. Lentivirus was produced in the University of California, San Francisco, Lentiviral RNAi Core. The day after infection, cells were seeded on to either plastic or gel substrates for 8 h before addition of selection media containing 2 μg/ml puromycin. After selection, TGFβ was added as indicated.

Western blot analysis

ATDC5 cells were serum starved (50/50 DMEM/F12, 0.2% fetal bovine serum [FBS]) for 4 h before treatment with TGFβ for 45 min. Whole-cell lysates were collected in 1× RIPA buffer (10 mM Tris, pH 8, 1 mM EDTA, 1 mM ethylene glycol tetraacetic acid, 140 mM sodium chloride, 1% Triton X-100, 0.1% sodium deoxycholate, 0.1% SDS) supplemented with 5 mM Na_3VO_4, 10 mM $NaPP_i$, 100 mM NaF, 500 μM phenylmethylsulfonyl fluoride, and 5 mg/ml eComplete Mini protease inhibitor tablet (11 836 153 001; Roche). Lysates were sonicated three times for 5 s each, clarified by centrifugation, and assessed for protein concentration using a Bradford assay. Protein was separated on 8.5% SDS–PAGE gels and transferred to nitrocellulose membranes. Blots were probed with the following primary and secondary antibodies: β-actin (ab8226; Abcam, Cambridge, MA), Smad2/3 (sc8332; Santa Cruz Biotechnology, Santa Cruz, CA), pSmad3 (a gift from E. Leof, Mayo Clinic, Rochester, MN), p38 (9218; Cell Signaling, Beverly, MA), pp38 (9211; Cell Signaling), and anti-mouse and anti-rabbit secondary antibodies that were conjugated to 680 or 800CW IRDye fluorophores detected using a LI-COR infrared imaging system (926-68020 and 926-32211; LI-COR Biosciences, Lincoln, NE). Blots shown are representative of multiple technical replicates of at least two independent experiments for each condition.

Immunofluorescence

Cells were cultured as indicated on collagen II–coated gel or glass substrates in eight-well Lab-Tek chamber slides (177402; Nunc/Thermo Fisher Scientific, Rochester, NY) with and without TGFβ for 45 min before harvest. Cells were washed in PBS twice, followed by fixation in 4% paraformaldehyde in PBS for 15 min at room temperature. After three PBS washes, cells were permeabilized in PBS with 0.5% Triton X-100 for 5 min and washed again (3× PBS). Cells were blocked for 1 h (PBS, 10% goat serum, and 0.5% Triton X-100) before overnight incubation with Smad2/3 antibody (sc8332; Santa Cruz Biotechnology) diluted 1:400 in PBS, 2% goat serum, and 3% Triton X-100 at 4°C in a humidifying chamber. After three PBS washes, cells were incubated with the secondary goat anti-rabbit Alexa Fluor 488 (A11034; Invitrogen) diluted 1:400 in PBS with 2% goat serum and 1.5% Triton X-100 for 1 h at room temperature, followed by another three washes with PBS. Rhodamine–phalloidin (R415; Invitrogen) was diluted to 1:800 in PBS and incubated with fixed cells for 20 min at room temperature. Finally, cells were washed with PBS three times and the well walls removed. For cells cultured on glass, the gasket was removed before adding SlowFade Gold mounting medium with 4′,6-diamidino-2-phenylindole (DAPI; S36939; Invitrogen) and covering it with a coverslip. For cells cultured on gels, the gasket was left attached, and mounting medium was added to each gel before applying the coverslip. Cells were visualized using an Olympus IX Widefield Microscope (Olympus, Tokyo, Japan). Images were processed in ImageJ (National Institutes of Health, Bethesda, MD). The averages and standard deviations shown in the figure represent the percentage of cells with nuclear localized Smad2/3 in several images taken across three biological replicates for each substrate. ANOVA followed by the Student Newman–Keuls test was used to evaluate statistical significance.

ACKNOWLEDGMENTS

We gratefully acknowledge V. Weaver and J. Lakins for sharing their expertise in the development of cell culture substrates with tunable stiffness, E. Leof for the phospho-Smad3 antibody, R. Marcucio for critical review of the manuscript, and the University of California, San Francisco, Lentiviral Core for their expertise and RNA interference services rendered. This research was supported by the University of California, San Francisco, Department of Orthopaedic Surgery, National Institutes of Health, National Institute of Dental and Craniofacial Research R01DE019284 (T.A.), a Howard Hughes Medical Institute Medical Research Fellowship (M.E.C.), and California Institute for Regenerative Medicine Training Grant TG2-01153 (J.A.). The contents of this publication are solely the responsibility of the authors and do not necessarily represent the official views of the California Institute for Regenerative Medicine or any other agency of the State of California.

REFERENCES

Aigner T, Kurz B, Fukui N, Sandell L (2002). Roles of chondrocytes in the pathogenesis of osteoarthritis. Curr Opin Rheumatol 14, 578–584.

Akizuki S, Mow VC, Muller F, Pita JC, Howell DS, Manicourt DH (1986). Tensile properties of human knee joint cartilage: I. Influence of ionic conditions, weight bearing, and fibrillation on the tensile modulus. J Orthop Res 4, 379–392.

Amano M, Chihara K, Kimura K, Fukata Y, Nakamura N, Matsuura Y, Kaibuchi K (1997). Formation of actin stress fibers and focal adhesions enhanced by Rho-kinase. Science 275, 1308–1311.

Annes JP, Munger JS, Rifkin DB (2003). Making sense of latent TGFbeta activation. J Cell Sci 116, 217–224.

Arany PR, Flanders KC, Kobayashi T, Kuo CK, Stuelten C, Desai KV, Tuan R, Rennard SI, Roberts AB (2006). Smad3 deficiency alters key structural elements of the extracellular matrix and mechanotransduction of wound closure. Proc Natl Acad Sci USA 103, 9250–9255.

Assoian RK, Klein EA (2008). Growth control by intracellular tension and extracellular stiffness. Trends Cell Biol 18, 347–352.

Balooch G *et al.* (2005). TGF-beta regulates the mechanical properties and composition of bone matrix. Proc Natl Acad Sci USA 102, 18813–18818.
Blaney Davidson EN, Remst DF, Vitters EL, van Beuningen HM, Blom AB, Goumans MJ, van den Berg WB, van der Kraan PM (2009). Increase in ALK1/ALK5 ratio as a cause for elevated MMP-13 expression in osteoarthritis in humans and mice. J Immunol 182, 7937–7945.
Blaney Davidson EN, van der Kraan PM, van den Berg WB (2007). TGF-beta and osteoarthritis. Osteoarthritis Cartilage 15, 597–604.
Butcher DT, Alliston T, Weaver VM (2009). A tense situation: forcing tumour progression. Nat Rev Cancer 9, 108–122.
Chang JL *et al.* (2010). Tissue-specific calibration of extracellular matrix material properties by transforming growth factor-beta and Runx2 in bone is required for hearing. EMBO Rep 11, 765–771.
Chen CS, Mrksich M, Huang S, Whitesides GM, Ingber DE (1997). Geometric control of cell life and death. Science 276, 1425–1428.
Clancy RM, Rediske J, Tang X, Nijher N, Frenkel S, Philips M, Abramson SB (1997). Outside-in signaling in the chondrocyte. Nitric oxide disrupts fibronectin-induced assembly of a subplasmalemmal actin/rho A/focal adhesion kinase signaling complex. J Clin Invest 100, 1789–1796.
Darling EM, Wilusz RE, Bolognesi MP, Zauscher S, Guilak F (2010). Spatial mapping of the biomechanical properties of the pericellular matrix of articular cartilage measured in situ via atomic force microscopy. Biophys J 98, 2848–2856.
Derynck R, Piek E, Schneider RA, Choy L, Alliston T (2008). TGF-beta family signaling in mesenchymal differentiation. In: The TGF-beta Family, ed. R Derynck, K Miyazono, Cold Spring Harbor, NY: Cold Spring Harbor Laboratory Press, 613–666.
Derynck R, Zhang YE (2003). Smad-dependent and Smad-independent pathways in TGF-beta family signalling. Nature 425, 577–584.
Discher DE, Janmey P, Wang YL (2005). Tissue cells feel and respond to the stiffness of their substrate. Science 310, 1139–1143.
Dong C, Li Z, Alvarez R Jr, Feng XH, Goldschmidt-Clermont PJ (2000). Microtubule binding to Smads may regulate TGF-beta activity. Mol Cell 5, 27–34.
Dupont S *et al.* (2011). Role of YAP/TAZ in mechanotransduction. Nature 474, 179–183.
Engler AJ, Sen S, Sweeney HL, Discher DE (2006). Matrix elasticity directs stem cell lineage specification. Cell 126, 677–689.
Feng XH, Filvaroff EH, Derynck R (1995). Transforming growth factor-beta (TGF-beta)-induced down-regulation of cyclin A expression requires a functional TGF-beta receptor complex. Characterization of chimeric and truncated type I and type II receptors. J Biol Chem 270, 24237–24245.
Furumatsu T, Tsuda M, Taniguchi N, Tajima Y, Asahara H (2005). Smad3 induces chondrogenesis through the activation of SOX9 via CREB-binding protein/p300 recruitment. J Biol Chem 280, 8343–8350.
Gao L, McBeath R, Chen CS (2010). Stem cell shape regulates a chondrogenic versus myogenic fate through Rac1 and N-cadherin. Stem Cells 28, 564–572.
Garamszegi N, Garamszegi SP, Samavarchi-Tehrani P, Walford E, Schneiderbauer MM, Wrana JL, Scully SP (2010). Extracellular matrix-induced transforming growth factor-beta receptor signaling dynamics. Oncogene 29, 2368–2380.
Geiger B, Spatz JP, Bershadsky AD (2009). Environmental sensing through focal adhesions. Nat Rev Mol Cell Biol 10, 21–33.
Gunnell LM, Jonason JH, Loiselle AE, Kohn A, Schwarz EM, Hilton MJ, O'Keefe RJ (2010). TAK1 regulates cartilage and joint development via the MAPK and BMP signaling pathways. J Bone Miner Res 25, 1784–1797.
Hansma P *et al.* (2009). The tissue diagnostic instrument. Rev Sci Instrum 80, 054303.
Haudenschild DR, Chen J, Pang N, Lotz MK, D'Lima DD (2010). Rho kinase-dependent activation of SOX9 in chondrocytes. Arthritis Rheum 62, 191–200.
Henderson JH, Carter DR (2002). Mechanical induction in limb morphogenesis: the role of growth-generated strains and pressures. Bone 31, 645–653.
Hinz B (2009). Tissue stiffness, latent TGF-beta1 activation, and mechanical signal transduction: implications for the pathogenesis and treatment of fibrosis. Curr Rheumatol Rep 11, 120–126.
Huang S, Ingber DE (2005). Cell tension, matrix mechanics, and cancer development. Cancer Cell 8, 175–176.
Ingber DE (2003). Mechanobiology and diseases of mechanotransduction. Ann Med 35, 564–577.
Kamaraju AK, Roberts AB (2005). Role of Rho/ROCK and p38 MAP kinase pathways in transforming growth factor-beta-mediated Smad-dependent growth inhibition of human breast carcinoma cells in vivo. J Biol Chem 280, 1024–1036.
Kanchanawong P, Shtengel G, Pasapera AM, Ramko EB, Davidson MW, Hess HF, Waterman CM (2010). Nanoscale architecture of integrin-based cell adhesions. Nature 468, 580–584.
Kiviranta P, Lammentausta E, Toyras J, Kiviranta I, Jurvelin JS (2008). Indentation diagnostics of cartilage degeneration. Osteoarthritis Cartilage 16, 796–804.
Kleemann RU, Krocker D, Cedraro A, Tuischer J, Duda GN (2005). Altered cartilage mechanics and histology in knee osteoarthritis: relation to clinical assessment (ICRS grade). Osteoarthritis Cartilage 13, 958–963.
Kumar D, Lassar AB (2009). The transcriptional activity of Sox9 in chondrocytes is regulated by RhoA signaling and actin polymerization. Mol Cell Biol 29, 4262–4273.
Leight JL, Wozniak MA, Chen S, Lynch ML, Chen CS (2012). Matrix rigidity regulates a switch between TGF-beta1-induced apoptosis and epithelial-mesenchymal transition. Mol Biol Cell 23, 781–791.
Li TF *et al.* (2010a). Aberrant hypertrophy in Smad3-deficient murine chondrocytes is rescued by restoring transforming growth factor beta-activated kinase 1/activating transcription factor 2 signaling: a potential clinical implication for osteoarthritis. Arthritis Rheum 62, 2359–2369.
Li Z, Dranoff JA, Chan EP, Uemura M, Sevigny J, Wells RG (2007). Transforming growth factor-beta and substrate stiffness regulate portal fibroblast activation in culture. Hepatology 46, 1246–1256.
Li Z, Kupcsik L, Yao SJ, Alini M, Stoddart MJ (2010b). Mechanical load modulates chondrogenesis of human mesenchymal stem cells through the TGF-beta pathway. J Cell Mol Med 14, 1338–1346.
Lin X, Liang M, Feng XH (2000). Smurf2 is a ubiquitin E3 ligase mediating proteasome-dependent degradation of Smad2 in transforming growth factor-beta signaling. J Biol Chem 275, 36818–36822.
Livak KJ, Schmittgen TD (2001). Analysis of relative gene expression data using real-time quantitative PCR and the 2(-Delta Delta C(T)) method. Methods 25, 402–408.
Maekawa M *et al.* (1999). Signaling from Rho to the actin cytoskeleton through protein kinases ROCK and LIM-kinase. Science 285, 895–898.
Massague J (1998). TGF-beta signal transduction. Annu Rev Biochem 67, 753–791.
Miranti CK, Brugge JS (2002). Sensing the environment: a historical perspective on integrin signal transduction. Nat Cell Biol 4, E83–E90.
Moriguchi T *et al.* (1996). A novel kinase cascade mediated by mitogen-activated protein kinase kinase 6 and MKK3. J Biol Chem 271, 13675–13679.
Mullen AC *et al.* (2011). Master transcription factors determine cell-type-specific responses to TGF-beta signaling. Cell 147, 565–576.
Munger JS, Sheppard D (2011). Cross talk among TGF-beta signaling pathways, integrins, and the extracellular matrix. Cold Spring Harb Perspect Biol 3, a005017.
Munger JS *et al.* (1999). The integrin alpha v beta 6 binds and activates latent TGF-beta 1: a mechanism for regulating pulmonary inflammation and fibrosis. Cell 96, 319–328.
Nofal GA, Knudson CB (2002). Latrunculin and cytochalasin decrease chondrocyte matrix retention. J Histochem Cytochem 50, 1313–1324.
Park JS, Chu JS, Tsou AD, Diop R, Tang Z, Wang A, Li S (2011). The effect of matrix stiffness on the differentiation of mesenchymal stem cells in response to TGF-beta. Biomaterials 32, 3921–3930.
Paszek MJ *et al.* (2005). Tensional homeostasis and the malignant phenotype. Cancer Cell 8, 241–254.
Qiao B, Padilla SR, Benya PD (2005). Transforming growth factor (TGF)-beta-activated kinase 1 mimics and mediates TGF-beta-induced stimulation of type II collagen synthesis in chondrocytes independent of Col2a1 transcription and Smad3 signaling. J Biol Chem 280, 17562–17571.
Reinhart-King CA, Dembo M, Hammer DA (2005). The dynamics and mechanics of endothelial cell spreading. Biophys J 89, 676–689.
Saeki K, Hilton JF, Alliston T, Habelitz S, Marshall SJ, Marshall GW, DenBesten P (2007). Elevated TGF-beta2 signaling in dentin results in sex related enamel defects. Arch Oral Biol 52, 814–821.
Sakai K, Mohtai M, Iwamoto Y (1998). Fluid shear stress increases transforming growth factor-beta 1 expression in human osteoblast-like cells: modulation by cation channel blockades. Calcif Tissue Int 63, 515–520.
Sasaki A, Masuda Y, Ohta Y, Ikeda K, Watanabe K (2001). Filamin associates with Smads and regulates transforming growth factor-beta signaling. J Biol Chem 276, 17871–17877.
Schuh E, Kramer J, Rohwedel J, Notbohm H, Muller R, Gutsmann T, Rotter N (2010). Effect of matrix elasticity on the maintenance of the chondrogenic phenotype. Tissue Eng Pt A 16, 1281–1290.

Seto H *et al*. (2004). Distinct roles of Smad pathways and p38 pathways in cartilage-specific gene expression in synovial fibroblasts. J Clin Invest 113, 718–726.
Setton LA, Elliott DM, Mow VC (1999). Altered mechanics of cartilage with osteoarthritis: human osteoarthritis and an experimental model of joint degeneration. Osteoarthritis Cartilage 7, 2–14.
Shieh AC, Athanasiou KA (2003). Principles of cell mechanics for cartilage tissue engineering. Ann Biomed Eng 31, 1–11.
Streuli CH, Schmidhauser C, Kobrin M, Bissell MJ, Derynck R (1993). Extracellular matrix regulates expression of the TGF-beta 1 gene. J Cell Biol 120, 253–260.
Thirion S, Berenbaum F (2004). Culture and phenotyping of chondrocytes in primary culture. Methods Mol Med 100, 1–14.
Tomasek JJ, Gabbiani G, Hinz B, Chaponnier C, Brown RA (2002). Myofibroblasts and mechano-regulation of connective tissue remodelling. Nat Rev Mol Cell Biol 3, 349–363.
van der Kraan PM, Blaney Davidson EN, Blom A, van den Berg WB (2009). TGF-beta signaling in chondrocyte terminal differentiation and osteoarthritis: modulation and integration of signaling pathways through receptor-Smads. Osteoarthritis Cartilage 17, 1539–1545.
Varelas X, Sakuma R, Samavarchi-Tehrani P, Peerani R, Rao BM, Dembowy J, Yaffe MB, Zandstra PW, Wrana JL (2008). TAZ controls Smad nucleocytoplasmic shuttling and regulates human embryonic stem-cell self-renewal. Nat Cell Biol 10, 837–848.
Wang G, Woods A, Sabari S, Pagnotta L, Stanton LA, Beier F (2004). RhoA/ROCK signaling suppresses hypertrophic chondrocyte differentiation. J Biol Chem 279, 13205–13214.
Wang JH, Thampatty BP (2006). An introductory review of cell mechanobiology. Biomech Model Mechanobiol 5, 1–16.
Wang YK, Yu X, Cohen DM, Wozniak MA, Yang MT, Gao L, Eyckmans J, Chen CS (2012). Bone morphogenetic protein-2-induced signaling and osteogenesis is regulated by cell shape, RhoA/ROCK, and cytoskeletal tension. Stem Cells Dev 21, 1176–1786.
Wells RG, Discher DE (2008). Matrix elasticity, cytoskeletal tension, and TGF-beta: the insoluble and soluble meet. Sci Signal 1, 13.
Williamson AK, Chen AC, Sah RL (2001). Compressive properties and function-composition relationships of developing bovine articular cartilage. J Orthop Res 19, 1113–1121.
Wipff PJ, Rifkin DB, Meister JJ, Hinz B (2007). Myofibroblast contraction activates latent TGF-beta1 from the extracellular matrix. J Cell Biol 179, 1311–1323.
Woods A, Beier F (2006). RhoA/ROCK signaling regulates chondrogenesis in a context-dependent manner. J Biol Chem 281, 13134–13140.
Woods A, Wang G, Beier F (2005). RhoA/ROCK signaling regulates Sox9 expression and actin organization during chondrogenesis. J Biol Chem 280, 11626–11634.
Wrana JL (2000). Regulation of Smad activity. Cell 100, 189–192.
Zawel L, Dai JL, Buckhaults P, Zhou S, Kinzler KW, Vogelstein B, Kern SE (1998). Human Smad3 and Smad4 are sequence-specific transcription activators. Mol Cell 1, 611–617.
Zhang Y, Chang C, Gehling DJ, Hemmati-Brivanlou A, Derynck R (2001). Regulation of Smad degradation and activity by Smurf2, an E3 ubiquitin ligase. Proc Natl Acad Sci USA 98, 974–979.